Linear Bending Analysis of a Pressurized Multicell Shell Structure

PAUL E. WILSON,* SANGIAH DHARMARAJAN,† AND PHILIP W. ROGERS‡
General Dynamics/Astronautics, San Diego, Calif.

An analysis of the stresses and deflections in the webs and partial cylinders of a uniformly pressurized multicell container of monocoque construction is presented. Linear bending theory of circular cylindrical shells serves as the basic mathematical model. Nondimensional closed-form solutions of the governing differential equations are presented, and by means of a parameter study, the over-all structural behavior of many tank geometries is evaluated numerically. Typical results reveal that 1) the discontinuity hoop bending stress is generally small compared to the hoop membrane stress, but tends to increase rapidly as the number of lobes increases; 2) it is possible to design a multicell tank such that the hoop bending stress will vanish identically; and 3) the radial web stress is large compared to the nominal hoop membrane stress and is consequently of considerable importance in design considerations.

Nomenclature

a = radius of partial cylinder
A_L = area of lobe cross section
b = radial distance from center of multicell tank to juncture of two partial cylinders
C = extensional rigidity coefficient, $C \equiv Eh/1 - \nu^2$
C_1,C_2 = nondimensional constants defined by Eqs. (12)
D = flexural rigidity, $D \equiv Eh^3/12(1 - \nu^2)$
E = modulus of elasticity, same for both web and partial cylinder
h = cylinder thickness
h_w = web thickness
H,V = stress resultants acting in positive (x,y) directions, respectively
M_ξ,M_z = hoop and axial stress couples, respectively
n = number of lobes
N_ξ,N_z = hoop and axial stress resultants, respectively
p = internal pressure
p_H,p_V = components of surface load intensity in positive (x,y) directions, respectively
Q = transverse shearing stress resultant
u,v = components of middle surface displacement in positive (x,y) directions, respectively
x,y,z = rectangular Cartesian coordinates
α = metric coefficient giving length of deformed shell along ξ coordinate line, $\alpha^2 \equiv (x')^2 + (y')^2$
β = rotation of a profile tangent
ϵ_ξ,ϵ_z = components of hoop and axial strain, respectively
$\epsilon_{\xi m},\epsilon_{zm}$ = components of hoop and axial membrane strain, respectively
ζ = distance from middle surface measured positive along inward directed normal
η = ratio of web to cylinder thickness, $\eta \equiv h_w/h$
θ = half-angle between two adjacent webs
ν = Poisson's ratio, for numerical work taken as 0.3
ξ = parameter defining x and y
ρ = cylinder radius-thickness ratio, $\rho \equiv a/h$
σ_ξ,σ_z = components of hoop and axial stress, respectively
$\sigma_{\xi b},\sigma_{zb}$ = components of hoop and axial bending stress, respectively
$\sigma_{\xi m},\sigma_{zm}$ = components of hoop and axial membrane stress, respectively
σ_w = radial stress in web
$\tau_{\xi\zeta}$ = transverse shearing stress
Φ = angle between y axis and normal to deformed middle surface
χ_ξ = hoop curvature change
ω = half-angle subtended by the partial cylinder
$(\ )'$ = derivative of quantity in parenthesis with respect to ξ
$(\ )_0$ = denotes that quantity in parenthesis is referred to the undeformed configuration

Introduction

RECENTLY interest has been renewed in the following question: As proposed launch and space vehicles keep getting larger, should they still be scaled-up versions of conventional circular cylindrical shell structures? Studies by NASA[1-3] imply that the use of multicell (instead of conven-

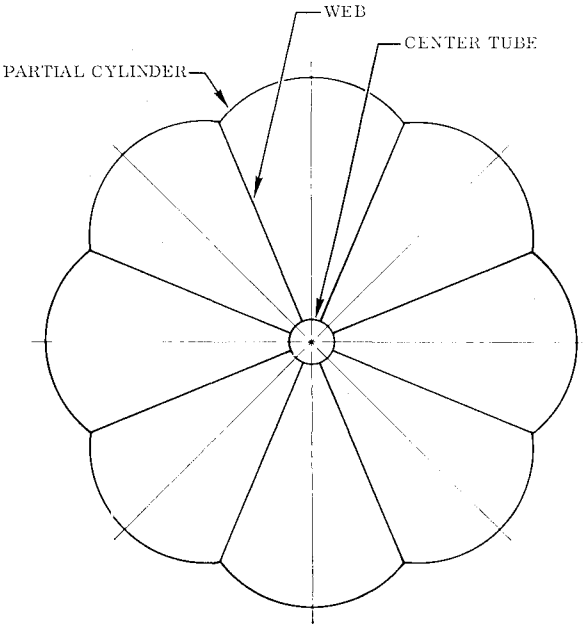

Fig. 1 Cross section of an eight-lobed multicell tank.

Received October 30, 1963; revision received November 23, 1964. Thanks are extended to A. H. Hausrath and R. T. Sullins for offering advice concerning certain aspects of this work. The authors also express appreciation to D. D. Taylor and E. M. Slick for providing programing support and appreciate the help given by L. M. Brock and M. T. Delaney in evaluating the numerical results.

* Design Specialist, Structures Research. Member AIAA.
† Consultant; also Associate Professor, School of Engineering, San Diego State College, San Diego, Calif.
‡ Senior Structures Engineer, Structures Research. Member AIAA.

tional cylindrical) structures looks promising. It is interesting to note that multicell configurations were recommended for space vehicles by Oberth[4] as early as 1929.

The cross section of a typical eight-lobe multicell tank is shown schematically in Fig. 1. The partial cylinders that form the tank periphery may be of monocoque, stiffened, or honeycomb construction. Stiffened webs extend radially from a center tube to the juncture of two outer wall sections and extend longitudinally between cell end closure bulkheads. The webs are perforated to allow pressure equalization between all lobes. Bulkheads are composed of partial truncated cones and spherical transition sections from the partial cones to the partial cylinders. Each radial web is attached to the outer partial cylinder juncture and to upper and lower adjacent bulkheads by means of extruded Y sections that are mechanically joined to the web and welded to the partial cylinders and bulkheads. Along the periphery of the cross section, the partial cylinders are attached to the spherical transition sections and to the skirt by means of partial Y sections. Because of sealing requirements, welding is employed for these attachments.

Advantages of multicell configurations over conventional circular cylindrical shapes stem primarily from the specific adaptability of multicell structures to various space vehicle requirements, and in this connection the following potential advantages have recently been suggested: 1) radial webs, already present as part of the basic structure, serve the dual purpose of slosh baffling; 2) large multicell boosters can be designed so that weldments require only single pass welds, whereas cylindrical boosters of comparable size require multiple pass welds; 3) multicell construction offers flexibility in selection of tank diameters and bulkhead arrangements, thereby making it possible to use existing facilities for manufacturing sections of a multicell vehicle; 4) for large space boosters, a comparison of multicell and cylindrical configurations for identical missions indicates that the multicell structure will be somewhat lighter and shorter; 5) with multicell construction it is possible to minimize fuel residuals, shorten skirt sections, optimize suction line locations, and obtain shorter and lighter thrust structures; 6) with appropriate use of mechanical connections, the radial webs may be fabricated from high-strength unweldable materials; and 7) the multicell concept can be adapted to lifting body shapes as needed for recoverable boosters.

The present paper contains an analysis of the stresses and deflections in the webs and partial cylinders of a multicell structure such as that shown schematically in Fig. 1. Sections in which the stresses and deflections are calculated are assumed to be somewhat removed from the end bulkheads. It is assumed that the structure is uniformly pressurized and of monocoque construction. Linear bending theory of circular cylindrical shells serves as the basic mathematical model. The governing differential equations are integrated and results of the analysis are arranged in suitable nondimensional form. A few typical results from a parametric study carried out on an IBM 7094 digital computer are given, and the more important findings are summarized.

Basic Equations for Cylinder

Analysis of Strain

Let a system of rectangular Cartesian coordinates (x, y, z) be oriented in a cylindrical shell (not necessarily circular) such that z is directed along a generator. Assume that the displacement components in the (x, y) directions are independent of z. Consequently, parametric equations of the deformed middle surface in a plane normal to the z axis (see Fig. 2) can be written in the form $x = x(\xi)$ and $y = y(\xi)$. By geometry it may be shown that

$$x' = \alpha \cos\Phi \qquad y' = \alpha \sin\Phi \tag{1}$$

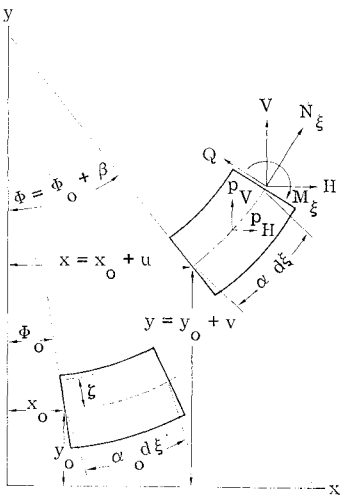

Fig. 2 Geometry of deformation, stress resultants, and components of middle surface loading intensity.

where primes denote differentiation with respect to ξ, Φ is the angle between the y axis and a normal to the deformed middle surface, and $\alpha^2 = (x')^2 + (y')^2$. With the Kirchhoff-Love hypothesis, along with the customary definition of engineering strain, it follows that the strain components $(\epsilon_\xi, \epsilon_z)$ can be written as follows:

$$\epsilon_\xi = \epsilon_{\xi m} + \zeta \chi_\xi \qquad \epsilon_z = \epsilon_{zm}$$

where

$$\epsilon_{\xi m} = \frac{\alpha}{\alpha_0} - 1 = \frac{x'}{x_0'} \frac{\cos\Phi_0}{\cos\Phi} - 1$$
$$\chi_\xi = \frac{(\Phi_0' - \Phi')}{\alpha_0} \tag{2}$$

Here ζ represents the distance from the middle surface measured positive along an inward directed normal, and the subscript 0 denotes quantities that refer to the undeformed configuration.

Stress Resultants

Let (σ_ξ, σ_z) represent the components of normal stress in the positive (ξ, z) directions, respectively, and denote the transverse shearing stress by $\tau_{\xi\zeta}$. Therefore with Eqs. (2) and Hooke's law

$$\epsilon_\xi = (\sigma_\xi - \nu\sigma_z)/E \qquad \epsilon_z = (\sigma_z - \nu\sigma_\xi)/E$$

along with the customary definitions of the stress resultants (N_ξ, N_z, Q) and stress couples (M_ξ, M_z)

$$(N_\xi, N_z, Q) = \int_{-h/2}^{h/2} (\sigma_\xi, \sigma_z, \tau_{\xi\zeta}) d\zeta$$

$$(M_\xi, M_z) = \int_{-h/2}^{h/2} (\sigma_\xi, \sigma_z) \zeta d\zeta$$

it follows that

$$N_\xi = C(\epsilon_{\xi m} + \nu\epsilon_{zm}) \qquad N_z = C(\epsilon_{zm} + \nu\epsilon_{\xi m})$$
$$M_\xi = D\chi_\xi \qquad M_z = \nu D\chi_\xi \tag{3}$$

where

$$C = Eh/1 - \nu^2 \qquad D = Eh^3/12(1 - \nu^2)$$

For what follows it is convenient to define additional stress resultants H and V (see Fig. 2) by the relations

$$N_\xi = H\cos\Phi + V\sin\Phi \qquad Q = -H\sin\Phi + V\cos\Phi \tag{4}$$

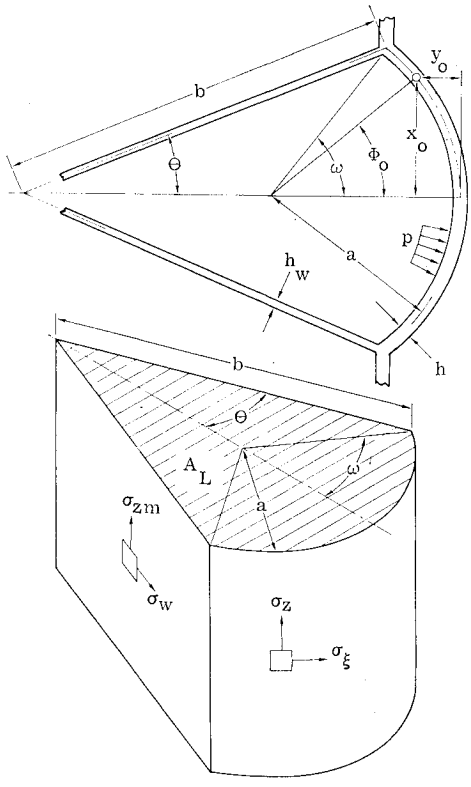

Fig. 3 Lobe geometry and stress states in web and partial cylinder.

Equilibrium Equations

Let (p_H, p_V) represent components of surface loading intensity that act in positive (x, y) directions, respectively. Accordingly, the differential equations of equilibrium of a deformed shell element become

$$H' + \alpha p_H = 0 \qquad V' + \alpha p_V = 0 \qquad M_\xi' - \alpha Q = 0 \tag{5}$$

Equations (1–5) are 12 equations in the 13 unknowns (x, y, Φ, α, $\epsilon_{\xi m}$, ϵ_{zm}, χ_ξ, N_ξ, N_z, M_ξ, H, V, and Q) which, along with a pertinent equilibrium equation resulting from summation of forces in the z direction, constitute a rather specialized theory of cylindrical shells that is valid for finite deflections. However, for the following, it is sufficient to restrict attention to the large class of problems that involve small membrane strains and rotations, viz., linear or small deflection theory.

Linear Theory

For purposes of linearization and reduction of the nonlinear equations, it is convenient to introduce displacement components (u, v) and a rotation β as follows (see Fig. 2):

$$x = x_0 + u \qquad y = y_0 + v \qquad \Phi = \Phi_0 + \beta$$

With these relations, appropriate linearization and reduction of Eqs. (1–5) yields the following system of five simultaneous linear differential equations:

$$\left.\begin{aligned} H' + \alpha_0 p_H &= 0 \qquad V' + \alpha_0 p_V = 0 \\ (D\beta'/\alpha_0)' &= \alpha_0(H \sin\Phi_0 - V \cos\Phi_0) \\ (u'/\alpha_0) &= -\beta \sin\Phi_0 + \\ &\quad (H \cos\Phi_0 + V \sin\Phi_0 - \nu N_z)(\cos\Phi_0/Eh) \\ v' &= (\alpha_0\beta + u' \sin\Phi_0)/\cos\Phi_0 \end{aligned}\right\} \tag{6}$$

When N_z is specified, Eqs. (6) may be solved for the basic dependent variables (u, v, β, H, V), and the stress components may be determined from the formulas

$$N_\xi = H \cos\Phi_0 + V \sin\Phi_0 \qquad M_\xi = -D\beta'/\alpha_0$$
$$M_z = \nu M_\xi \tag{7}$$
$$(\sigma_\xi, \sigma_z) = (N_\xi, N_z)/h + 12\zeta(M_\xi, M_z)/h^3$$

Analysis

Tank Geometry

The idealized cross section of a typical lobe (or cell) of a proposed multicell tank is shown in Fig. 3. The outer periphery of each lobe is a portion of a thin circular cylindrical shell. Webs consisting of flat plates extend radially from a common center juncture point to the intersection of two cylindrical sections. It is assumed that the structure is entirely of monocoque construction. Accordingly, the geometry of a cross section is completely specified when θ, ω, a, h, and h_w are given. In general there are n lobes; consequently $\theta = \pi/n$. Also, from the geometry of Fig. 3, $b = a \sin\omega/\sin\theta$. It should be noted that ω is not completely arbitrary, i.e., in view of geometric constraints, the only admissible values of ω must satisfy the inequality $\theta \leq \omega \leq \theta + (\pi/2)$.

Calculation of Axial Stress

Each cell is subjected to a uniform internal pressure p as shown in Fig. 3. It is assumed that the longitudinal membrane stress σ_{zm} is constant and the same in both the webs and partial cylinders, and the web is assumed to be in a membrane stress state as shown in Fig. 3. Admittedly, these assumptions are open to question. However, owing to the choice of load paths, they should serve as a reasonable first approximation. Consequently, if A_L is the area of the cross section of a typical lobe, axial equilibrium of the entire multicell container cross section requires that

$$pnA_L = \sigma_{zm} n(bh_w + 2a\omega h)$$

or

$$\sigma_{zm} = N_z/h = paC_1/h \tag{8a}$$

where

$$C_1 = \frac{\omega + \sin^2\omega \cot\theta - \sin\omega \cos\omega}{2\omega + (h_w/h)(\sin\omega/\sin\theta)} \tag{8b}$$

Equations for Circular Cylinder

Parametric equations of the undeformed middle surface of the cylinder (Fig. 3) may be written in the form $x_0 = a \sin\Phi_0$ and $y_0 = a(1 - \cos\Phi_0)$. Hence, it is convenient to select $\xi = \Phi_0$ and $\alpha_0 = a$. The surface loading is such that $p_H = p \sin\Phi_0$ and $p_V = -p \cos\Phi_0$. Consequently, for a shell of constant thickness, Eqs. (6) reduce immediately to the form

$$\left.\begin{aligned} H' &= -pa \sin\Phi_0 \qquad V' = pa \cos\Phi_0 \\ (D\beta''/a^2) &= H \sin\Phi_0 - V \cos\Phi_0 \\ (u'/a) &= -\beta \sin\Phi_0 + \\ &\quad (H \cos\Phi_0 + V \sin\Phi_0 - \nu paC_1)(\cos\Phi_0/Eh) \\ v' &= (a\beta + u' \sin\Phi_0)/\cos\Phi_0 \end{aligned}\right\} \tag{9}$$

Equations (9) comprise a sixth-order system of differential equations; hence it is necessary to prescribe six boundary-juncture conditions. Five of these conditions result from symmetry, viz.,

$$u(0) = \beta(0) = \beta(\omega) = V(0) = v(\omega) + u(\omega) \cot\theta = 0 \tag{10a}$$

Also, equilibrium and symmetry at the juncture of a web and two partial cylinders require that

$$[u(\omega)/a]\,\csc\omega = (1/E)(\sigma_w - \nu\sigma_{zm})$$

$$\sigma_w h_w = 2[V(\omega)\cos\theta - H(\omega)\sin\theta]$$

Accordingly, by eliminating σ_w, the necessary juncture condition can be put in the form

$$[u(\omega)/a]\,\csc\omega = (1/Eh)\{(2h/h_w)[V(\omega)\cos\theta - H(\omega)\sin\theta] - \nu paC_1\} \quad (10b)$$

Integration and Numerical Results

The solution of Eqs. (9) subject to the boundary-juncture equations (10) requires only elementary quadratures. Results of this procedure, suitably grouped so that only fundamental nondimensional parameters appear, are summarized as follows:

$$\left.\begin{aligned}
&\frac{H}{pa} = C_2 + \cos\Phi_0 \qquad \frac{V}{pa} = \sin\Phi_0\\
&\frac{\beta}{pa^3/Eh^3} = 12\,C_2(1-\nu^2)\left(\frac{\Phi_0}{\omega}\sin\omega - \sin\Phi_0\right)\\
&\frac{u}{pa^2/Eh} = (1-\nu C_1)\sin\Phi_0 + \frac{C_2}{2}\left(\Phi_0 + \frac{1}{2}\sin 2\Phi_0\right) - 6C_2\rho^2(1-\nu^2)\times\\
&\left[2\frac{\sin\omega}{\omega}(\sin\Phi_0 - \Phi_0\cos\Phi_0) - \left(\Phi_0 - \frac{1}{2}\sin 2\Phi_0\right)\right]\\
&\frac{v}{pa^2/Eh} = (1-\nu C_1)(\cos\omega - \cos\Phi_0 - \sin\omega\cot\theta) - \frac{C_2}{2}[1 - 12\rho^2(1-\nu^2)](\sin^2\omega - \sin^2\Phi_0) - \frac{C_2}{2}\left(\omega + \frac{1}{2}\sin 2\omega\right)\cot\theta + 12\,C_2\rho^2(1-\nu^2)\times\\
&\left[\frac{\sin\omega}{\omega}(\cos\Phi_0 - \cos\omega + \Phi_0\sin\Phi_0 - \omega\sin\omega) + \left(\frac{\sin^2\omega}{\omega} - \frac{1}{4}\sin 2\omega - \frac{\omega}{2}\right)\cot\theta\right]
\end{aligned}\right\} \quad (11)$$

where

$$\left.\begin{aligned}
C_1 &= \frac{\omega + \sin^2\omega\cot\theta - \frac{1}{2}\sin 2\omega}{2\omega + \eta\,(\sin\omega/\sin\theta)}\\
C_2 &= \frac{\sin(\omega-\theta) - \frac{1}{2}\eta}{\sin\theta + \frac{\eta}{4}\left(\frac{\omega}{\sin\omega} + \cos\omega\right) + 3\,\eta\,\rho^2(1-\nu^2)\times\left(\frac{\omega}{\sin\omega} + \cos\omega - 2\frac{\sin\omega}{\omega}\right)}\\
&\rho = a/h \qquad \eta = h_w/h
\end{aligned}\right\} \quad (12)$$

In addition, the pertinent components of membrane and bending stress can be written in the form

$$\left.\begin{aligned}
&\frac{\sigma_{\xi m}}{pa/h} = 1 + C_2\cos\Phi_0\\
&\frac{\sigma^{\xi}_b}{pa/h} = \pm 6C_2\rho\left(\cos\Phi_0 - \frac{\sin\omega}{\omega}\right) \text{ for } \zeta = \pm\frac{h}{2}\\
&\frac{\sigma_{zm}}{pa/h} = C_1 \qquad \frac{\sigma_{zb}}{pa/h} = \nu\frac{\sigma_{\xi b}}{pa/h}\\
&\frac{\sigma_w}{pa/h} = \frac{2}{\eta}[\sin\omega\cos\theta - (C_2 + \cos\omega)\sin\theta]
\end{aligned}\right\} \quad (13)$$

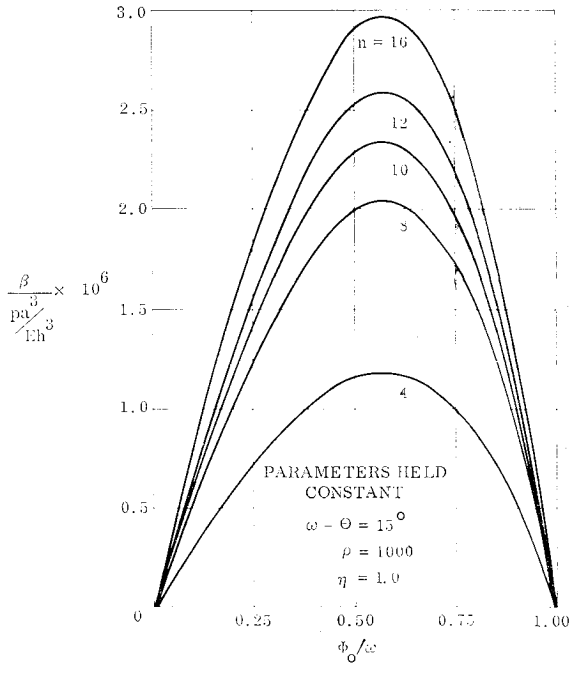

Fig. 4 Nondimensional rotation vs Φ_0/ω with n as a parameter.

Note that all stress components have been normalized with respect to the nominal membrane hoop stress (i.e., pa/h) in the partial cylinders.

Parametric evaluation of the over-all structural behavior of the pressurized multicell tank was carried out for suitable ranges of the dimensionless geometric parameters, viz., $n = 4, 8, 10, 12, 16$; $\omega - \theta = 0°, 15°, 30°, 45°, 60°, 75°, 90°$; $\rho = 500, 750, 1000, 1250, 1500$; and $\eta = 0.5, 1.0, 1.5, 2.0, 2.5$. These values encompass a majority of the geometric configurations presently being proposed for aerospace applications. By means of a digital computer, the nondimensional components of displacement and stress were computed for each combination of the geometric parameters. Complete numerical results are too extensive to present here in detail, but typical results are given and the more interesting findings are summarized.

Typical plots of the nondimensional rotation, displacement, and inner surface bending stress vs Φ_0/ω are shown in Figs. 4–6. In constructing these graphs, the number of lobes n was allowed to vary from 4–16, the other geometric parameters assumed the constant values $\omega - \theta = 15°$, $\rho = 1000$, and $\eta = 1.0$. Note that for this set of geometries the bending stress is maximum at the juncture $\Phi_0 = \omega$, and increases rapidly as n increases. In this instance, the bending stress in the partial cylinder is only a small percentage of the nominal hoop stress pa/h. Also, for this set of configurations, as well as all other geometries considered here, the membrane stress in the partial cylinder is essentially constant and for all practical purposes equal to pa/h. Results shown in Fig. 7 are also of interest. The nondimensional inner surface bending stress is plotted vs Φ_0/ω for various η holding $n = 12$, $\omega - \theta = 30°$, and $\rho = 1000$. Observe that the inner surface bending stress at the discontinuity $\Phi_0 = \omega$ changes sign

depending on the value of η, and that $\sigma_{\xi b}$ is identically zero for $\eta = 1$. In fact, within the framework of the present theory, it may be seen by inspection that the bending stress in the partial cylinder vanishes identically for all Φ_0 if $\omega - \theta = \sin^{-1}(\eta/2)$ where $\eta \leq 2$, which suggests the interesting possibility of designing a multicell structure that experiences membrane stresses only.

Information given in Fig. 8 is of considerable practical importance. Here the nondimensional inner surface bending stress in the partial cylinder at $\Phi_0 = \omega$ is plotted vs $\omega - \theta$ for various n with $\rho = 1000$ and $\eta = 1.0$. For these parameters, the plot shows that the bending stress becomes quite important as n increases and $(\omega - \theta) \to 0$. In particular, for $n = 16$, $\Phi_0 = \omega = \theta = 11.25°$, $\rho = 500$, and $\eta = 0.5$, data from the digital computer output indicate that $\sigma_{\xi b}$ becomes as large as $0.42\ pa/h$.

A typical plot of the nondimensional axial membrane stress vs $\omega - \theta$ for various values of n is shown in Fig. 9. Notice that σ_{zm} generally tends to increase as $\omega - \theta$ increases. In Fig. 10 the nondimensional radial stress in the web is plotted vs $\omega - \theta$ for various values of η. The web stresses are surprisingly large and consequently are of considerable importance in the design of the multicell structure under consideration. Observe that σ_w varies inversely with η and inincreases with increasing $\omega - \theta$. For cases considered here, the web stress is as large as four times the nominal hoop stress in the partial cylinder.

Concluding Remarks

The present analysis has certain limitations. Shearing stresses in the webs and partial cylinders are not accounted for, axial strains in the webs and partial cylinders are incompatible at the juncture $\Phi_0 = \omega$, and the assumptions made in computing σ_{zm} are open to question. More rigorous analyses to be carried out in the future should be devoted to resolving these discrepancies. In addition, hydrostatic pressure and axial, bending, and sloshing loads should ulti-

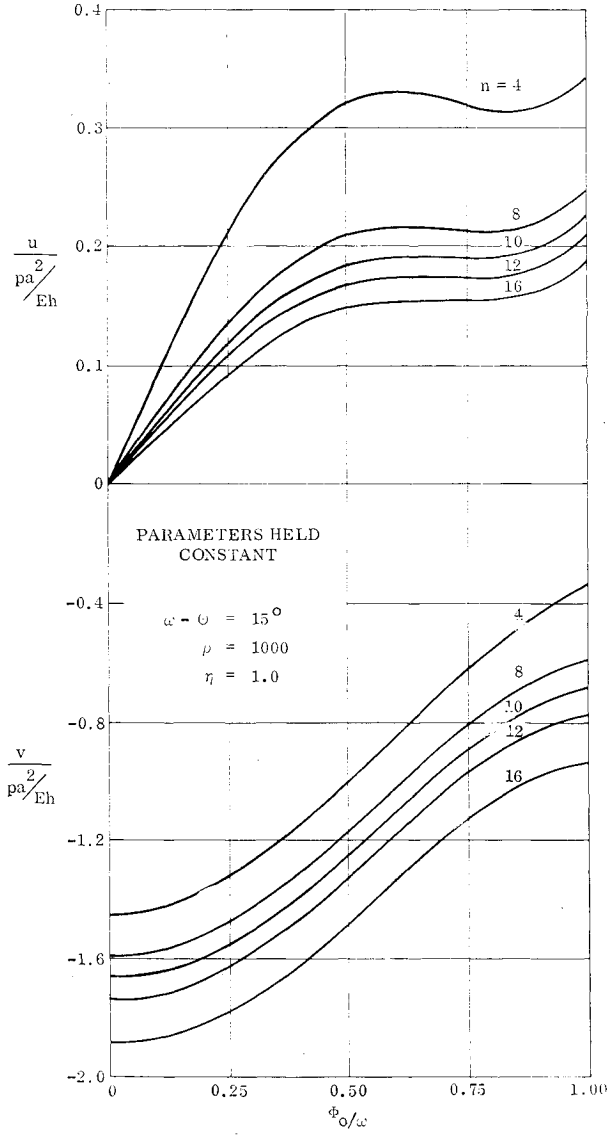

Fig. 5 Nondimensional displacement components in x and y directions vs Φ_0/ω with n as a parameter.

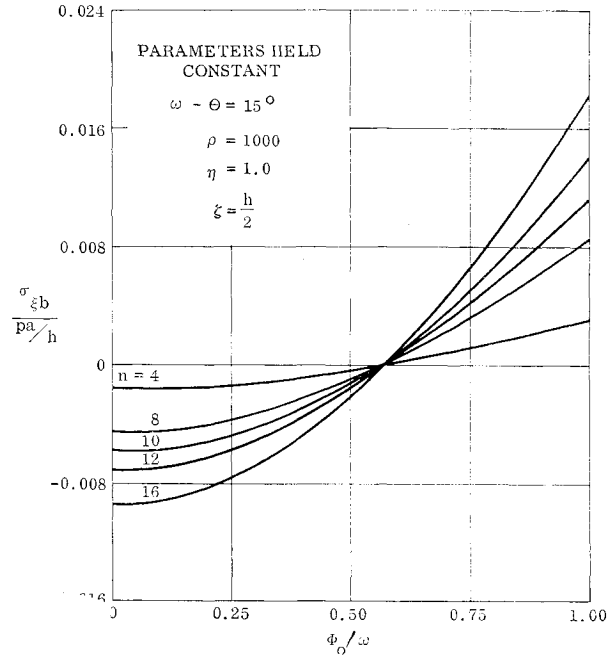

Fig. 6 Nondimensional hoop bending stress vs Φ_0/ω with n as a parameter.

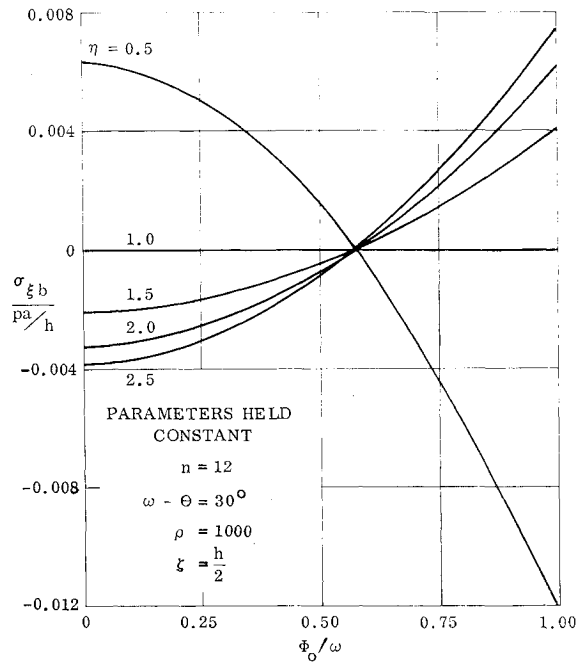

Fig. 7 Nondimensional hoop bending stress vs Φ_0/ω with η as a parameter.

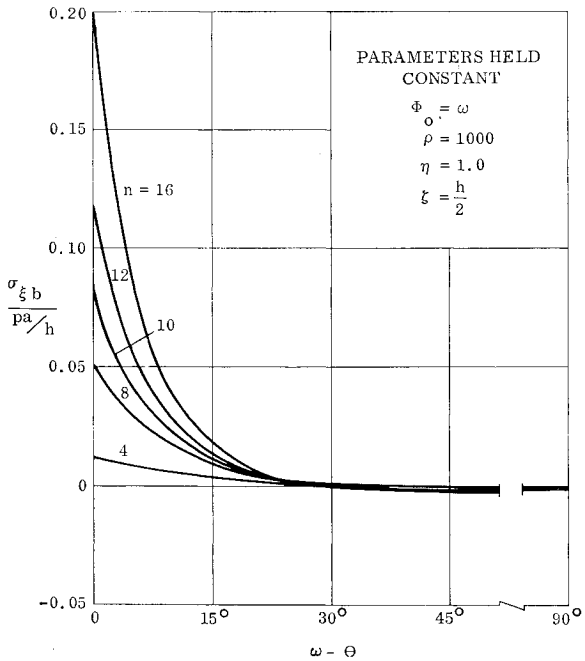

Fig. 8 Nondimensional hoop bending stress vs $\omega - \theta$ with η as a parameter.

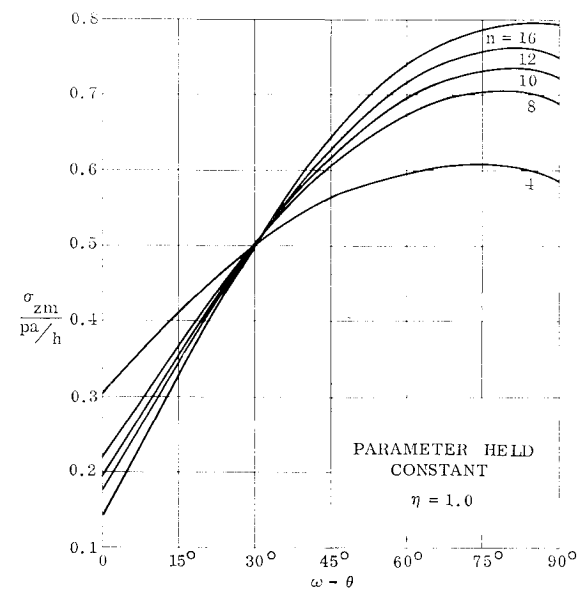

Fig. 9. Nondimensional longitudinal membrane stress vs $\omega - \theta$ with n as a parameter.

mately be considered. Questions concerning buckling, thermal stress, pressure coupling, variable thickness, and stiffened construction should also be investigated. In spite of these limitations, it is felt that the information presented here will give the engineer added insight into the design of multicell shell structures. The present analysis should serve as a reasonable first approximation to the solution of the multicell tank problem, and should help point the way to future research in this problem area.

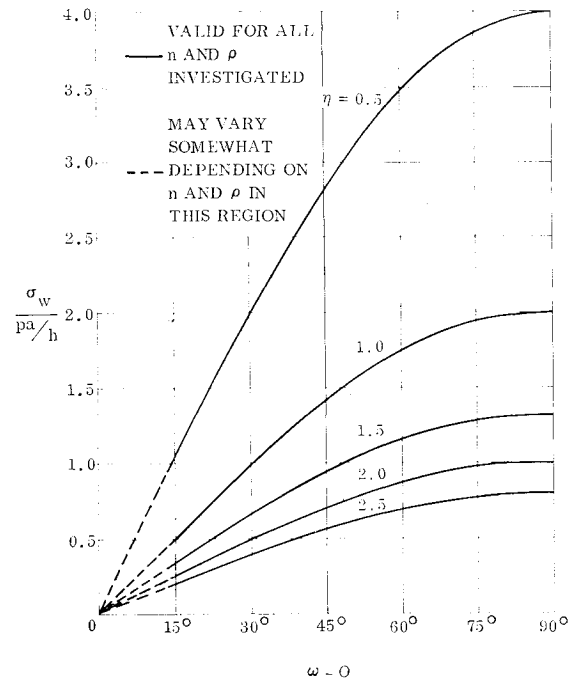

Fig. 10 Nondimensional radial web stress vs $\omega - \theta$ with η as a parameter.

The analysis technique used here has been previously discussed in more detail in a General Dynamics/Astronautics report.[5] Also, the basic calculation scheme employed in this paper closely parallels Reissner's approach[6] to the analysis of large axisymmetric deformation of shells of revolution. In fact, when the equations given in Ref. 6 are linearized and specialized to the limiting case of a toroidal shell such that a pertinent mean radius of revolution approaches infinity, the resulting equations are essentially those given by Eqs. (9). It should be pointed out that the problem considered here may also be solved by a suitable adaptation of an analysis of the stresses in a spoked flywheel.[7]

References

[1] Blumrich, J. F., "Multicell vs. cylindrical booster," NASA Marshall Space Flight Center, Internal Note IN-P & VE-SA-62-10, Huntsville, Ala. (July 1962).

[2] Blumrich, J. F., "Multi-cell structures studied for large boosters," Space/Aeronautics **39**, 86–89 (January 1963).

[3] "Integrated manufacturing plan 200-inch multicell test tank," NASA Marshall Space Flight Center, Procedure EP-6007, Huntsville, Ala. (December 1962).

[4] Oberth, H., *Wege zur Raumschiffahrt* (R. Oldenbourg, München, Germany, 1929), 3rd ed., Chap. 7, pp. 44–54.

[5] Wilson, P. E., Dharmarajan, S., and Rogers, P. W., "Linear bending analysis of a pressurized multicell shell structure," General Dynamics/Astronautics Rept. GD/A 63-0968, ERR-AN-336 (September 1963).

[6] Reissner, E., "On the theory of thin elastic shells," *Reissner Anniversary Volume* (J. W. Edwards Brothers, Inc., Ann Arbor, Mich., 1949), pp. 231–247.

[7] Timoshenko, S., *Strength of Materials* (D. Van Nostrand Co., Inc , New York, 1941), 2nd ed., Chap. 2, pp. 98–101.